Inflammation, Vol. 44, No. 1, February 2021 (© 2020)
DOI: 10.1007/s10753-020-01311-z

ORIGINAL ARTICLE

Sprouty2 Inhibits Migration and Invasion of Fibroblast-Like Synoviocytes in Rheumatoid Arthritis by Down-regulating ATF2 Expression and Phosphorylation

Xing Zhang,[1] Dongmei Zhang,[2] Qinyu Wang,[1] Xiaofeng Guo,[1] Jiajia Chen,[1] Jiawei Jiang,[1] Mengmeng Li,[2] Wei Liu,[1] Yingying Gao,[3] Qi Zhang,[4] Guofeng Bao,[1,5] and Zhiming Cui[1,5]

Abstract—Activating transcription factor 2(ATF2), a transcription factor belonging to the AP-1 family, plays an important role in inflammation. However, its biological functions and underlying molecular mechanisms in rheumatoid arthritis (RA) remain unclear. Western blot and immunohistochemistry were used to identify the expression of ATF2 and Sprouty2(SPRY2) in RA synovial tissues. SW982 cells were stimulated by TNF-α to establish an *in vitro* RA fibroblast-like synoviocyte (RA-FLS) model. Transwell and monolayer wound-healing were used to detect cell migration and invasion. RNA interference (si-ATF2) and adenovirus vector (Ad-SPRY2) methods were employed to manipulate ATF2 or SPRY2 expression in SW982 cells. The protein expression and phosphorylation levels in SW982 cells were evaluated by western blot. ATF2 expression and phosphorylation were upregulated in the RA synovial tissues. In RA-FLS model, ATF2 expression and phosphorylation were increased in a time-dependent manner. ATF2 knockdown inhibited the migration and invasion of RA-FLS model,

Xing Zhang and Dongmei Zhang contributed equally to this work.

Electronic supplementary material The online version of this article (https://doi.org/10.1007/s10753-020-01311-z) contains supplementary material, which is available to authorized users.

[1] Department of Orthopedics, The Second Affiliated Hospital of Nantong University, No. 6 Haier Lane North Road, Nantong, 226001, Jiangsu Province, People's Republic of China
[2] Medical Research Center, The Second Affiliated Hospital of Nantong University, Nantong, 226001, Jiangsu Province, People's Republic of China
[3] Department of Rheumatology, The Second Affiliated Hospital of Nantong University, 226001, Jiangsu ProvinceNantong, People's Republic of China
[4] The Jiangsu Key Laboratory of Neuroregeneration, Nantong University, Nantong, 226001, Jiangsu Province, People's Republic of China
[5] To whom correspondence should be addressed at Department of Orthopedics, The Second Affiliated Hospital of Nantong University, No. 6 Haier Lane North Road, Nantong, 226001, Jiangsu Province, People's Republic of China. E-mails: baodianone@163.com; zhimingcui@126.com

reducing the inflammatory factors, which was consistent with the influence on cell behaviors caused by SPRY2 overexpression. Moreover, SPRY2 overexpression inhibited the TNF-α-induced phosphorylation of ERK and ATF2 in SW982 cells. The high expression and phosphorylation of ATF2 promoted migration and invasion of RA-FLSs. SPRY2 might inhibited the inflammatory responses of RA-FLSs *via* suppressing ERK-ATF2 pathway.

KEY WORDS: rheumatoid arthritis; fibroblast-like synoviocytes; ATF2; SPRY2; ERK MAPK; inflammation.

INTRODUCTION

Rheumatoid arthritis (RA) is a chronic inflammatory disease featured by joint damage resulted from synovial inflammation. Complexed risk factors such as immune disorders, external environmental exposure, and genetic background regulation synergistically contribute to the onset of RA [1–3]. The pathological changes characterized by synovitis inflammation, hyperplasia, bone, and cartilage destruction cause a poor prognosis of RA [4]. Profiting by its powerful migration and invasion capabilities similar to tumor cells, activated RA-fibroblast-like synoviocytes (RA-FLSs) directly promote the generation and development of three basic RA lesions accompanied by the release of multiple pro-inflammatory factors including interleukin-6 (IL-6), IL-1β, reactive oxygen species (ROS), and matrix metalloproteinases (MMPs) [5, 6]. Therefore, studies on repression of RA-FLS activation have been extensively carried out recently.

As a classic inflammatory signaling pathway, ERK MAPK signaling pathway has been discovered to be over-activated in RA-FLS cells [7, 8]. Our previous studies indicated that Sprouty2 (SPRY2) can inhibit ERK MAPK signaling pathway and thus restrain RA-FLS activation [9]. SPRY2, a subfamily member of sprouty protein, negatively regulates several key tyrosine kinase and thus curbs cell proliferation and invasion in different tumors [10–12]. Moreover, SPRY2 overexpression prevented inflammatory factor production of FLSs [13].

ATF2, a defined downstream target of ERK MAPK cascade, belongs to the activator protein-1 (AP-1) transcription factor family. ATF2 consists of a transcription activation domain (TAD), an N′-terminal zinc finger (ZnF), and a basic leucine zipper (bzip) domain. In response to the stimulation of various extracellular stresses including ultraviolet ray (UV), ROS, and inflammatory cytokines, the two threonine residues (Thr69 and Thr71) of ATF2 are subsequently phosphorylated, which leads to ATF2 activation [14, 15]. Although traditional studies implicated that ATF2 promoted tumorigenesis by increasing proliferation and invasion of cancer cells [16, 17], recent evidence pointed out the role of ATF2 in inflammation. Our previous study revealed that ATF2 promoted the release of inflammatory cytokines in lipopolysaccharide-induced BV2 microglial cells and mediated neuronal apoptosis [18]. Interestingly, two latest studies implied a potential pro-inflammatory activity of ATF2 in both peripheral blood mononuclear leukocytes and FLSs of RA [19, 20]. Unfortunately, testimony manifesting ATF2 involved in the pathological process of RA is insufficient, and the underlying regulatory mechanism remains unclear.

In this study, we discovered the natural expression and over-activation of ATF2 in synovial tissues of RA patients, probed the effects of ATF2 and SPRY2 on the migration and invasion of TNF-α-induced SW982 cells *in vitro*, and further explored their relationship in RA-FLSs and potential mechanisms involved in RA pathogenesis.

MATERIALS AND METHODS

Patients and Tissue Samples

Human synovial tissues were obtained from eight RA patients who underwent total knee or total hip arthroplasty in the Department of Orthopedics, Affiliated Hospital 2 of Nantong University. The synovial tissues from eight healthy individuals isolated during arthroscopic surgery were used as control. The age of RA patients was 49 ± 6.3 years and in the control group was 45 ± 5.6 years. The study was approved by the institutional medical ethics committee of Affiliated Hospital 2 of Nantong University, and informed consents were acquired from all patients prior to surgery.

Cell Culture and Stimulation

Synovial tissues were washed 5 times with PBS (Gibco, USA) and cut into 2–3 mm pieces, then digested with collagenase II (Sigma, USA) in DMEM (Gibco, USA) for 2 h at 37 °C. After subcultured with 0.25% trypsin solution (Sigma, USA), the cells were incubated in DMEM (Gibco, USA) containing 10% FBS (Gibco,

USA), 100 U/ml penicillin, and 100 μg/ml streptomycin (Hyclone, Australia) at 37 °C with 5% CO_2. Cells were used for experiments at passages of third to six.

The human synovial cell line SW982 was purchased from Shanghai Zhong Qiao Xin Zhou Biotechnology Co., Ltd., China. These cells were cultured in DMEM containing 10% FBS, 100 U/ml penicillin, and 100 μg/ml streptomycin in air containing 5% CO_2 at 37 °C. The medium was changed every 2 days, and the cells were passaged once the cell fusion degree was above 90%. When conducting *in vitro* experiments in SW982 cells, the cells were incubated with DMEM containing 2% FBS for 24 h, and then stimulated with the specified concentration of TNF-α for a certain period of time, and the cells were harvested for subsequent experiments.

Immunohistochemical Analysis

Fresh synovial tissues were fixed with 4% paraformaldehyde at 4 °C overnight, then embedded in paraffin and cut into 5-μm sections. The sections were soaked in xylene three times for 10 min, dehydrated with different concentrations of ethanol, rinsed with water, restored antigen with sodium citrate, added endogenous peroxidase blocker for 30 min, then incubated with anti-ATF2 (1:100, CST, USA) or anti-SPRY2 (1:100, Abcam, USA) overnight at 4 °C, followed by incubation with respective horseradish peroxidase (HRP)-conjugated secondary antibodies (1:400, Abcam, USA) for 30 min at room temperature. The sections were stained with DAB, then hydrochloric acid color-separation for 3–5 min. After counterstaining with hematoxylin for 20–30 s, rinsing with running water for 10 min, repeat the dehydration step. Finally, air-dry the sections and seal. The stained sections were observed by microscope (Zeiss axio imager m2, Germany).

Immunofluorescence Cell Staining

RA-FLSs were seeded on sterile glass coverslips in 24-well plates, fixed in 4% paraformaldehyde for 20 min, then block for 1–2 h with Triton-containing immunostaining blocking solution (Beyotime, China). Next, immunostained with anti-ATF2 (1:80, CST, USA) or anti-Vimentin (1:100, Beyotime, China) antibodies overnight at 4 °C, followed by incubation Alexa 488 nm and 594 nm conjugated secondary antibody. Nuclei were stained by DAPI (Beyotime, China) and viewed under microscope (Zeiss axio imager m2, Germany).

Western Blot Analysis

Cells and homogenized tissues were lysed in the lysis buffer (RIPA Potent lysate: PMSF = 100:1) for 30 min at 0–4 °C. The supernatant was collected after centrifugation, which heated with loading buffer at 100 °C for 5–8 min. The samples were subjected to 10–12% SDS-PAGE and then transferred to PVDF membranes (Millipore). After blocking for 2 h with skim milk, probed with the primary antibody as follows: anti-ATF2 (1:1000, CST, USA), anti-p-ATF2 (1:800, CST, USA), anti-SPRY2 (1:1000, Abcam, USA), anti-GAPDH (1:1000 Beyotime, China), anti-ERK, anti-pho-ERK (1:500, Sangon Biotech, China), anti-MMP-13 (1:800, Sangon Biotech, China), and anti-IL-1β (1:500, Sangon Biotech, China). The membrane was visualized after incubating with anti-mouse/anti-rabbit HRP-conjugated second antibody for 2 h at room temperature.

Enzyme-Linked Immunosorbent Assay

The medium supernatant of different groups of pretreated cells was measured with IL-6 enzyme-linked immunosorbent assay (ELISA) kit (CUSABIO, China), and processed data according to the manufacturer's instructions. The absorbance at 450 nm was read by a microplate reader (BioTek Instruments, Inc., USA).

Transwell Invasion Assay

Configure the SW982 cell suspension with DMEM (without FBS; with or without TNF-α) until the final concentration is 5×10^5/ml. Slowly add 200 μl cell suspension to a pre-coated Matrigel (BD Biosciences, UK) upper transwell chamber, which later put into the bottom chamber containing 800 μl DMEM medium with 10% FBS. Cells on the bottom membrane of the chamber were fixed with 4% paraformaldehyde and stained with 0.1% crystal violet after 12 h of incubation. Randomly select 5 clear fields under the microscope for counting.

Monolayer Wound-Healing Assays

SW982 cells were seeded into 6-well plates at a concentration of 2×10^5/well. When the cells reach 80% confluence, wounds were scratched by sterile pipette trips (200 μl type). Then add 2 ml DMEM containing 1% FBS after rinsing off the unattached cells with PBS, and TNF-α was added to the experimental group medium to a final concentration of 10 ng/ml. After

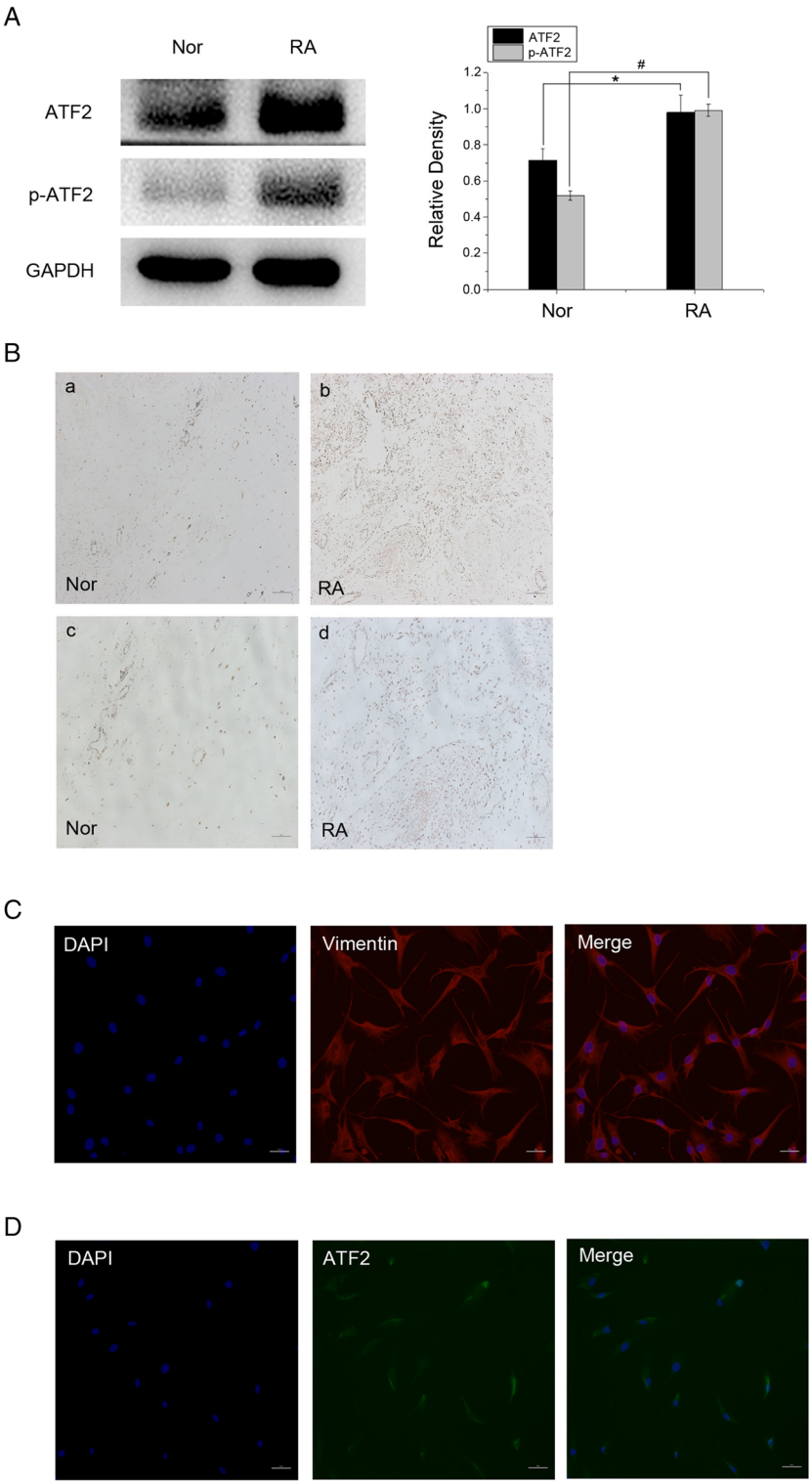

Fig. 1. Up-regulated expression and activation of ATF2 in synovial tissues of RA patients. **a** Western blot assay was employed to determine the expression of ATF2 and p-ATF2 in synovial tissues of RA patients and healthy controls. **b** Immunohistochemical detection of ATF2: control (left); RA (right). **c**–**d** Immunofluorescence cell staining was used to detect the localization of Vimentin (red) and ATF2 (green) in the isolated RA-FLSs. Data were represented as the mean of three different experiments. $*P < 0.05$, compared with healthy controls.

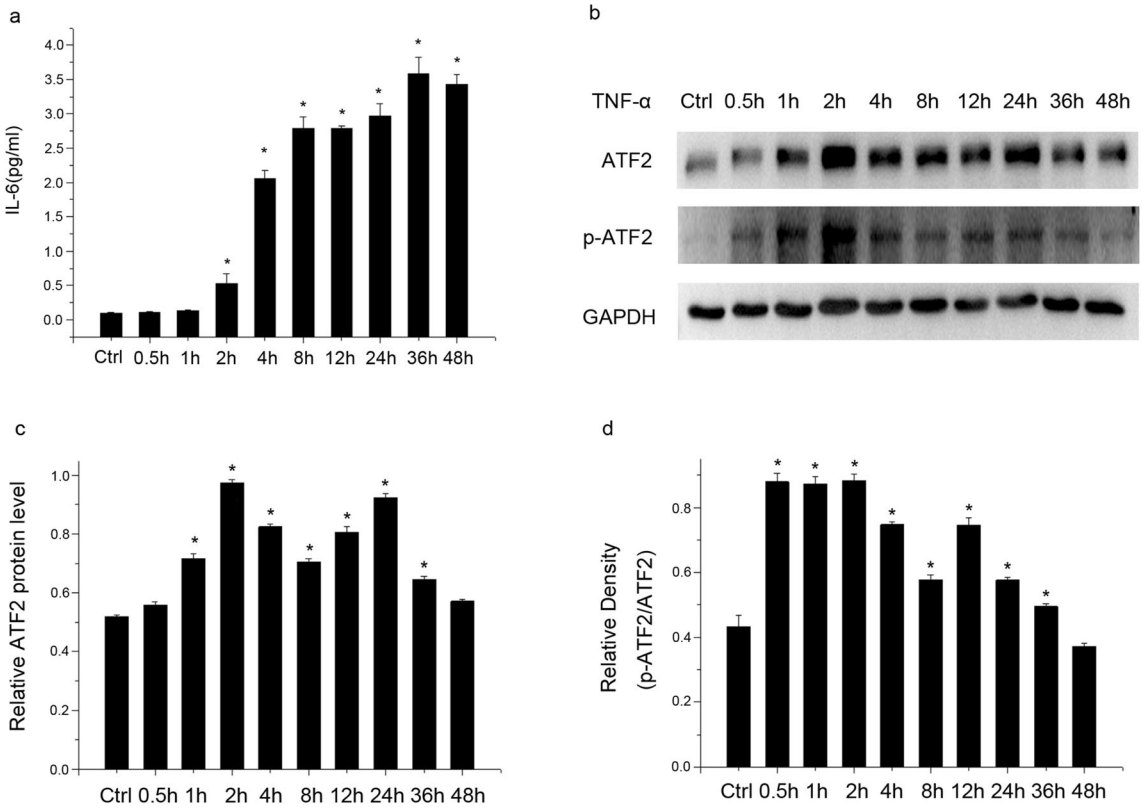

Fig. 2. Increased ATF2 expression and activation in TNF-α-stimulated SW982 cells. **a** The level of IL-6 in SW982 cell medium supernatant was detected by ELISA kits. **b**–**d** SW982 cells were stimulated with TNF-α (10 ng/ml) for 0 h, 0.5 h, 1 h, 2 h, 4 h, 8 h, 12 h, 24 h, 36 h, and 48 h. The protein levels of ATF2 and p-ATF2 were measured by western blot. Upper blot showed ATF2 and p-ATF2 protein levels; lower blot demonstrated equal loading respectively by detecting GAPDH and ATF2. The values shown are mean ± SEM of data from three independent experiments. (*$P < 0.05$ significant compared with control alone).

incubation, take pictures of wounds on the same site at different time points including 0 h, 12 h, 24 h, 36 h, and 48 h to assess cell migration.

SiRNA and Transfection

Human ATF2 siRNA and si-Ctrl (negative control) were purchased from Hanbio, China. According to the manufacturer's recommendations, RNAFit (Hanbio, China) was used to facilitate transient transfection of siRNA. The complexes formulated with siRNA or si-Ctrl and RNAFit, which were used to transfect cells will be replaced by total medium after 2 h. The treated cells were then cultured at 37 °C and used for subsequent experiments 48 h later.

Expression of Ad-SPRY2

Recombinant Ad-SPRY2 adenovirus and Ad-GFP (negative control) were purchased from Hanbio China. SW982 cells (5×10^5/well) were cultured in 6-well plates, which infected with different multiplicities of infection (MOI) of Ad-SPRY2 (Hanbio China) and Ad-GFP. The transfection efficiency of Ad-SPRY2 and Ad-GFP were verified by both western blot and its fluorescent tags. Vintage MOI was selected based on both transfection efficiency and cytotoxicity. SW982 cells transfected at least for 48 h were suitable for constructing cell models for further experiments.

Statistical Analysis

All statistical analysis was performed with SPSS software version 19.0 (IBM, Chicago, IL, USA). The data were expressed as the mean ± standard deviation. The differences between each group detected by *t* tests, and $P < 0.05$ in all cases were considered to be statistically significant.

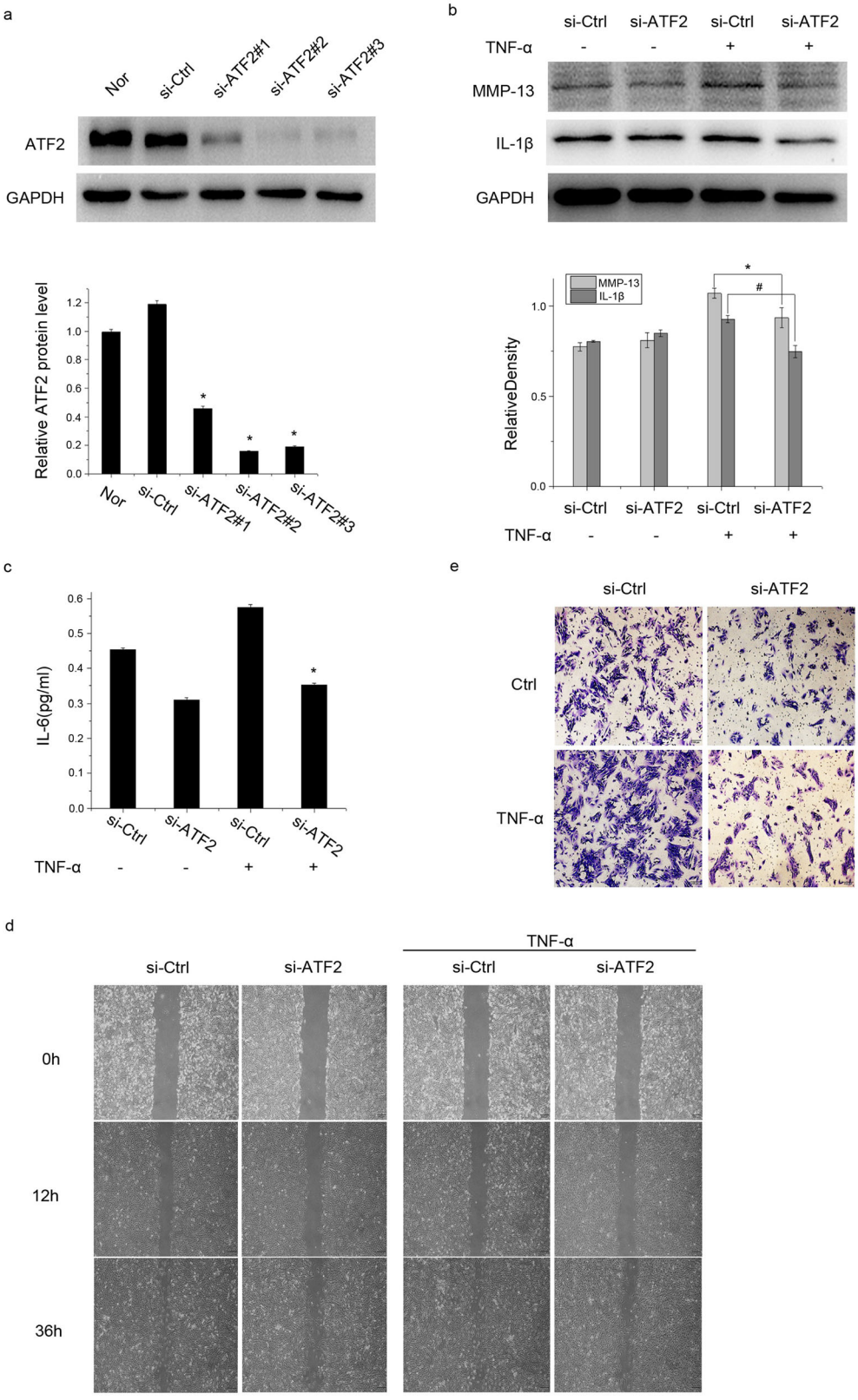
a
Nor
si-Ctrl
si-ATF2#1
si-ATF2#2
si-ATF2#3
ATF2
GAPDH
Relative ATF2 protein level
b
si-Ctrl
si-ATF2
si-Ctrl
si-ATF2
TNF-α
MMP-13
IL-1β
GAPDH
MMP-13
IL-1β
RelativeDensity
c
IL-6(pg/ml)
si-Ctrl
si-ATF2
si-Ctrl
si-ATF2
TNF-α
e
si-Ctrl
si-ATF2
Ctrl
TNF-α
d
TNF-α
si-Ctrl
si-ATF2
si-Ctrl
si-ATF2
0h
12h
36h

◀ **Fig. 3.** ATF2 knockdown attenuated the migration and invasion of TNF-α treated SW982 cells. **a** Three different siRNAs against ATF2 (si-ATF2) were used to transfect SW982 cells. The transfection efficiency was evaluated by Western blot assay. The scrambled siRNA was used as a negative control (si-Ctrl). Si-ATF2#3 was used for the following experiment. **b** Western blot indicated that inhibition of ATF2 suppressed the protein expression of IL-β and MMP-13 in SW982 cells stimulated by TNF-α (10 ng/ml). **c** ELISA was used to verify the IL-6 expression in SW982 cell supernatant. Data showed that ATF2 knockdown inhibited IL-6 level with or without TNF-α stimulation. **d** The migration ability of SW982 cells was evaluated by the monolayer wound-healing assay. **e** Transwell assay was performed to assess SW982 cells invasion. All results are representatives of at least three repeated experiments.

RESULTS

Up-regulated Expression and Activation of ATF2 in Synovial Tissues of RA Patients

To evaluate the potential involvement of ATF2 in RA, western blot assay was used to detect the expression and activation of ATF2 in the synovial tissues of RA patients and healthy individuals. ATF2 expression and phosphorylation (p-ATF2) were both increased significantly in RA synovial tissues compared with healthy controls (Fig. 1a). Immunohistochemistry assay confirmed ATF2 overexpression in synovial sections of RA patients than healthy controls (Fig. 1b). Moreover, cellular immunofluorescence staining revealed a detectable basal level of ATF2 protein in FLSs isolated from synovial tissues of RA patients (Fig. 1d). Immunostaining of Vimentin was used as a special marker of FLSs (Fig. 1c).

Increased ATF2 Expression and Activation in TNF-α-Stimulated SW982 Cells

To further explore the function of ATF2 in RA-FLSs, we stimulated SW982 cells with TNF-α (10 ng/ml) to construct a RA-FLSs activation model *in vitro*. ELISA indicated that the supernatant levels of pro-inflammatory factor IL-6 increased sharply in a time-dependent manner and peaked at 36 h in SW982 cells after TNF-α treatment (Fig. 2a). Then, western blot revealed the expression of ATF2 significantly elevated in TNF-α-stimulated SW982 cells in a time-dependent manner and reached the maximum at 2 h and 24 h (Fig. 2b, c). Meanwhile, the level of ATF2 phosphorylation also enhanced by TNF-α and peaked at 0.5 h 1 h and 2 h (Fig. 2d).

ATF2 Knockdown Attenuated the Migration and Invasion of TNF-α Treated SW982 Cells

To evaluate the biological function of ATF2 in the pathogenesis of RA, we knocked down ATF2 expression in SW982 cells by RNA interfering (siRNA). The knockdown efficiency was verified by western blot assay (Fig. 3a), and si-ATF2#3 was used for the following experiment. Compared with the negative control (si-Ctrl) group, SW982 cells transfected with si-ATF2 produced much lower amounts of MMP-13 and IL-1β with or without TNF-α treatment (Fig. 3b). Inhibiting ATF2 expression also decreased IL-6 production in TNF-α stimulated SW982 cells, which indicated by ELISA assay (Fig. 3c). Monolayer wound-healing assays indicated that ATF2 knockdown suppressed SW982 cells invasion after TNF-α stimulation (Fig. 3d). Concurrently, transwell migration assay showed that TNF-α treatment obviously increased the migration of SW982 cells, whereas si-ATF2 significantly decreased this phenomenon (Fig. 3e).To avoid non-specific effects, we also performed the above functional assays using si-ATF2#1 and obtained similar results, which further proved a pro-inflammatory function of ATF2 in RA-FLSs (Fig. S1).

Expression of SPRY2 in Synovial Tissues and TNF-α-Stimulated SW982 Cells

To further elucidate the underlying molecular mechanism, we next explore the possible upstream cascades. In accordance with previous findings, western blot determined a much higher protein expression of SPRY2, an important inhibitor of ERK MAPK, in synovial tissues of healthy persons than in RA patients (Fig. 4a). This observation was further verified by immunohistochemistry assay (Fig. 4b). In SW982 cells, the expression of SPRY2 increased tardily following the administration of TNF-α, reached the peak at 12 h, and decreased sharply thereafter (Fig. 4d).

SPRY2 Overexpression Inhibited the Invasion and Migration of TNF-α Treated SW982 Cells

We next overexpressed SPRY2 in SW982 cells *via* adenovirus vector. After infected with 300 MOI Ad-GFP for 48 h, most cells expressed detectable GFP (Fig. 5a). Although SW982 cells in 1000 MOI group expressed more GFP proteins, massive cell died due to adenovirus cytotoxicity. The dose 300 MOI was determined for further

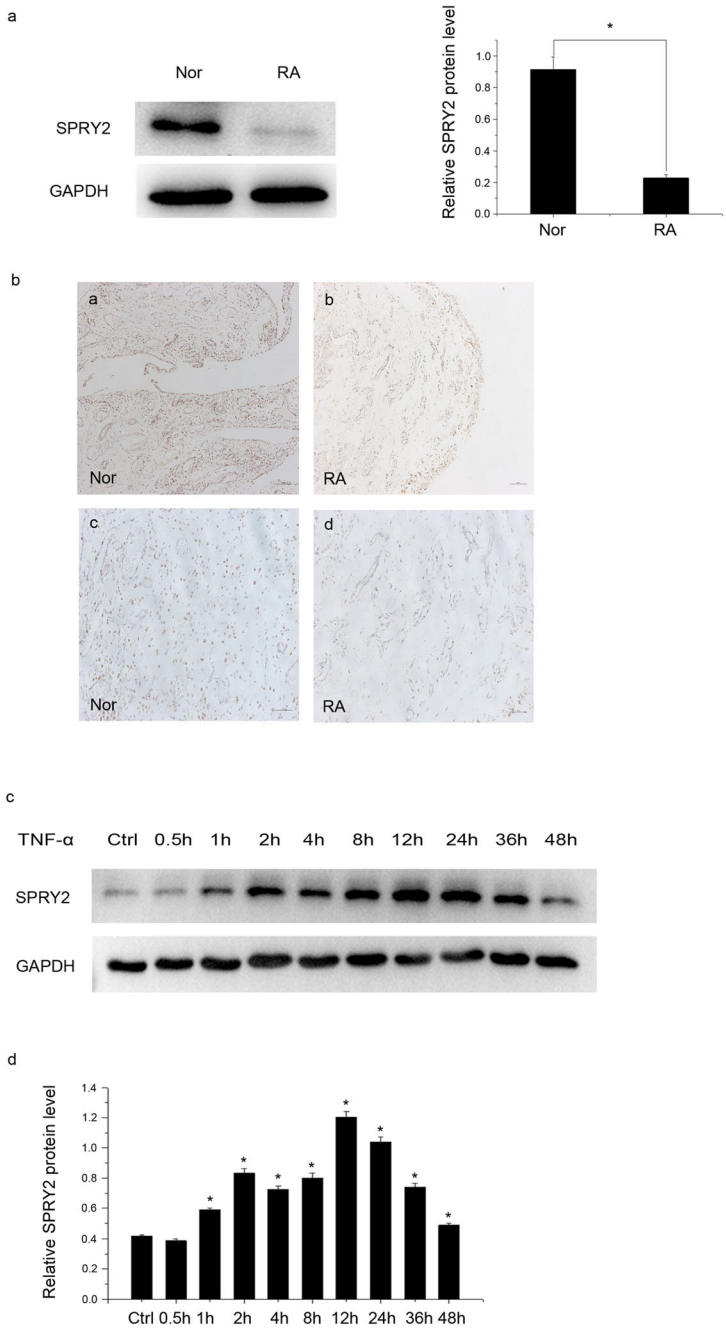

Fig. 4. Expression of SPRY2 in synovial tissues and TNF-α-stimulated SW982 cells. **a** Western blot was used to analyzed the SPRY2 expression in rheumatoid synovial tissues. **b** Immunohistochemical analysis of SPRY2 expression in the synovial tissues of the control group and the RA patients. **c**–**d** SPRY2 expression was measured by western blot assay, while SW982 cells were stimulated by TNF-α (10 ng/ml) for 0 h, 0.5 h, 1 h, 2 h, 4 h, 8 h, 12 h, 24 h, 36 h, and 48 h; lower blot demonstrated equal loading by detecting GAPDH. All data were displayed as mean ± SD, $^{*}P < 0.05$.

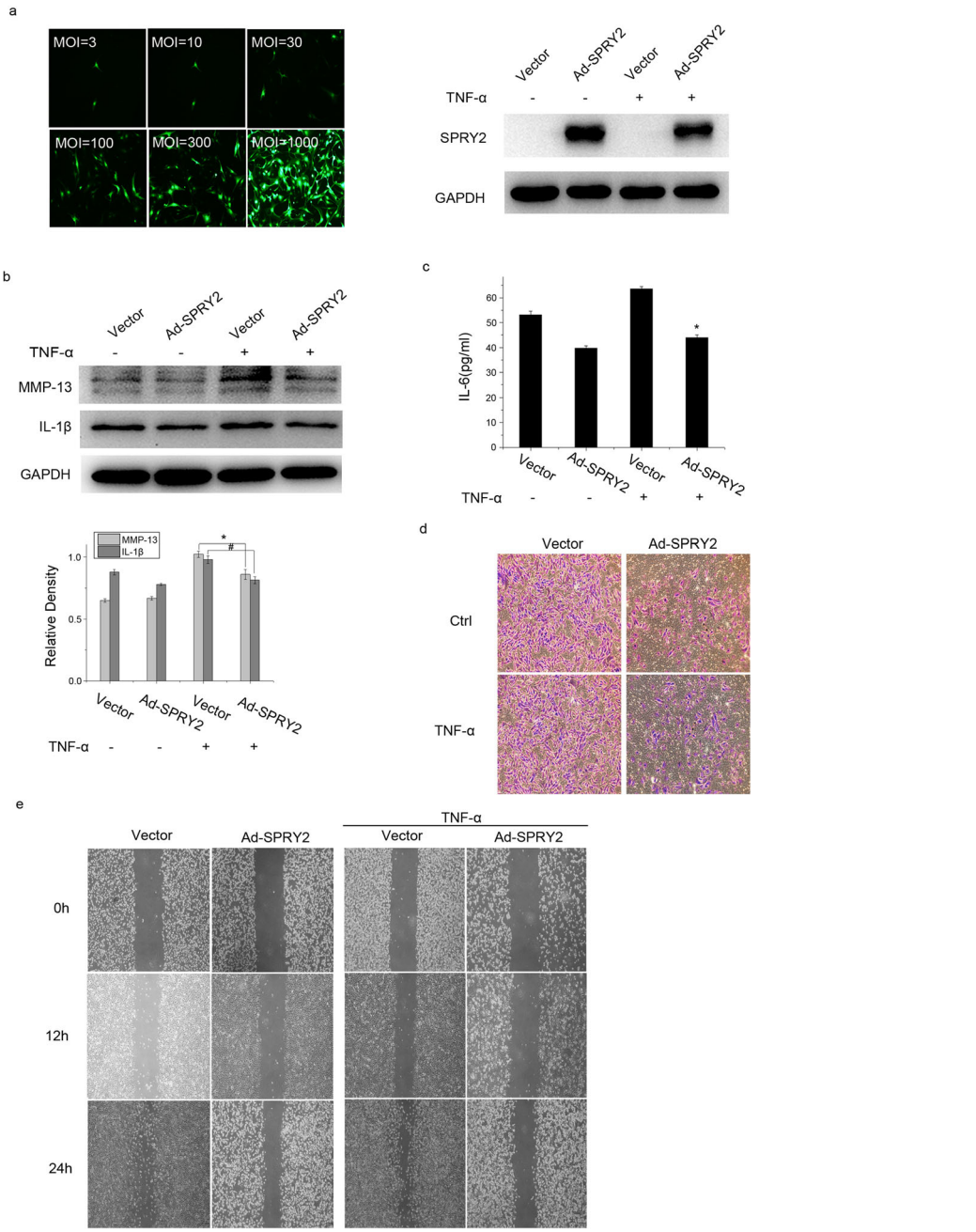

Fig. 5. SPRY2 overexpression inhibited the invasion and migration of TNF-α treated SW982 cells. **a** Observation of SW982 cells infected with AdGFP (green) of MOI at 300 under immunofluorescence microscopy (× 10). Western blot analysis obtained from SW982 cells infected with 300 MOI of AdSPRY2 as indicated. **b** MMP-13 and IL-1β protein expression in TNF-α (10 ng/ml) treatment was measured by western blot assay. **c** ELISA was used to analysis the IL-6 expression. **d** We carried out invasion assay in a Matrigel basement membrane matrix chamber, then counted invaded cells. **e** We detected migration ability of SW982 cells by wound-healing assays. $*P < 0.05$.

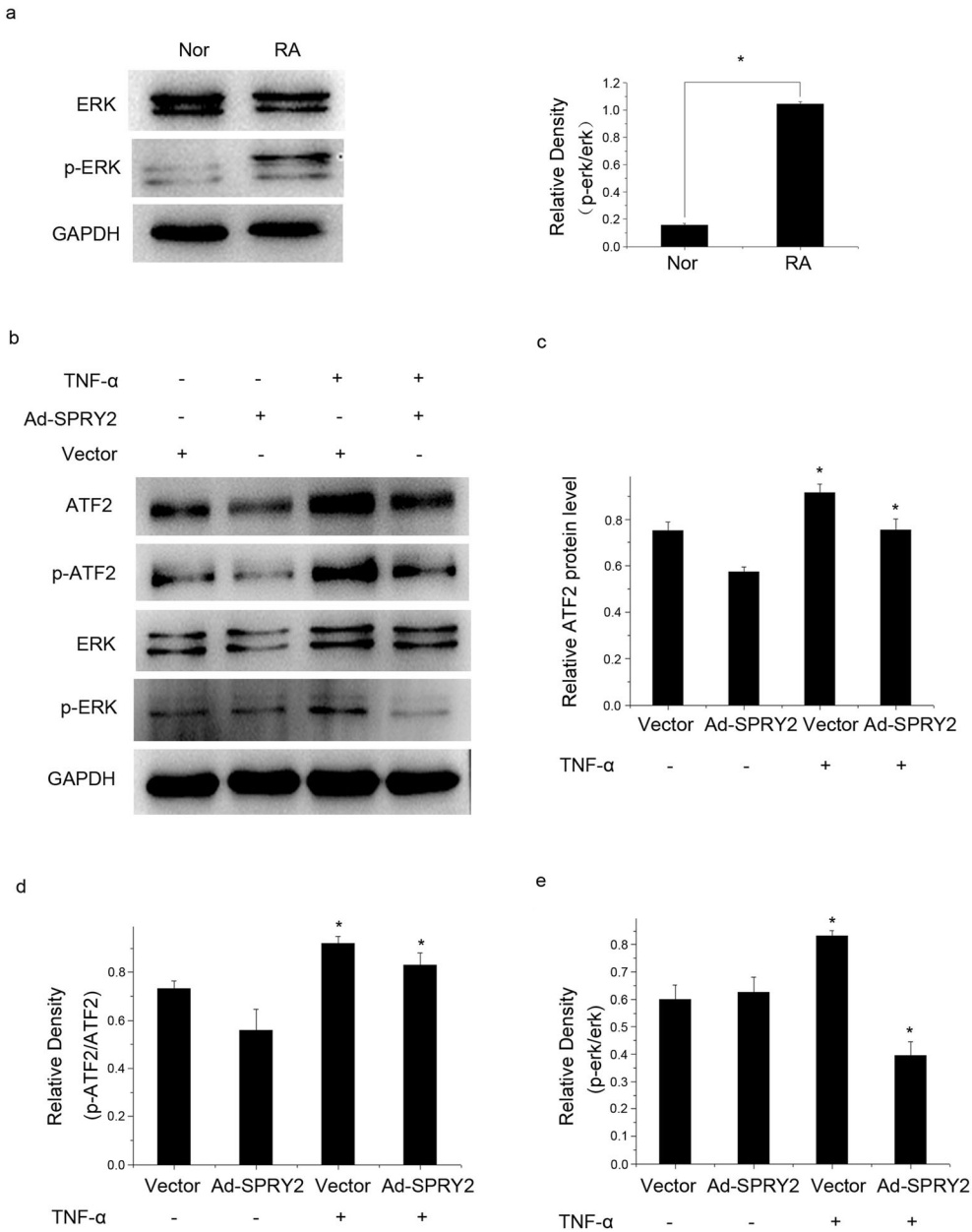

Fig. 6. SPRY2 inhibits expression and phosphorylation of ATF2 by repressing ERK signal pathway in SW982 cells. **a** The protein level of ERK and p-ERK in rheumatoid synovial tissues was measured by Western blot. **b** SW982 cells were treated with 10 ng/ml TNF-α for periods indicated. The phosphorylated level of ATF2 and ERK in whole cell lysates was analyzed by western blot, using total ATF2 and total ERK as the controls. **c**–**e** Western blot analysis was conducted to assess the mean fold change of ATF2/GAPDH, p-ATF2/ATF2, and p-ERK/ERK. Compared with untreated control cells, $*P < 0.05$.

experiments in view of the results. Western blot assay confirmed the significant overexpression of SPRY2 protein in Ad-SPRY2 group than control group whether stimulated by TNF-α or not (Fig. 5a). Immunoblotting analysis confirmed that the protein expression levels of MMP-13 and IL-1β in the Ad-SPRY2 group were significantly lower than those of the control group regardless of whether they were stimulated by TNF-α (Fig. 5b). ELISA detected lower expression of IL-6 in Ad-SPRY2-treated SW982 cells (Fig. 5c). Transwell assay indicated that the invasion

ability of SW982 cells was largely prevented by Ad-SPRY2 (Fig. 5d). We also observed that Ad-SPRY2 inhibited SW982 cells migration, as examined by scrap-wound migration assay (Fig. 5e).

SPRY2 Inhibits Expression and Phosphorylation of ATF2 by Repressing ERK Signal Pathway in SW982 Cells

A plenty of studies reported that the activation of ATF2 in inflammation can be facilitated by ERK MAPK pathway; previous researches supported that SPRY2 plays a protective role in RA *via* inhibiting the activation of ERK MAPK. In order to further investigate the potential mechanism through which SPRY2 inhibits the activation of FLSs, we evaluated the regulation of SPRY2 on ATF2 and its upstream ERK MAPK signaling pathway. Western blot explored that phosphorylated ERK (p-ERK), an active form of ERK, was highly expressed in synovial tissues of RA patients compared with healthy group (Fig. 6a). TNF-α elevated the phosphorylation of ERK (p-erk) and ATF2 (p-ATF2) in SW982 cells (Fig. 6b); however, the ERK/ATF2 phosphorylation was significantly attenuated by SPRY2 overexpression (Ad-SPRY2) (Fig. 6c, d, e). In summary, our data indicated that ATF2 activation may be suppressed by SPRY2 *via* inhibiting ERK MAPK signaling pathway in SW982 cells.

DISCUSSION

Rheumatoid arthritis is a systemic autoimmune disease, characterized by inflammatory synovitis [4, 21]. Hyperactive migration and invasion of activated FLSs directly promote the destruction of articular and bone, resulting in RA progression [5, 22, 23]. In the present experiment, we demonstrated an increased expression of ATF2 in synovial tissues of RA patients and revealed a proinflammatory function of ATF2 in TNF-α stimulated SW982 cells. We also implied the existence of SPRY2-ERK MAPK-ATF2 axis in RA-FLSs.

ATF2 belongs to both AP-1 and bZIP families and plays a significant role in cellular stress responses. Ubiquitously, ATF2 expresses throughout the mammalian body whose function is frequently regulated by JNK/P38/ERK MAPK signaling pathways [24–26]. Originally, investigations on ATF2 were mainly among tumor diseases. For example, increased expression of ATF2/phospho-ATF2/phospho-ERK was detected in bladder tumors and was positively correlated with poor prognosis. Knocking down ATF2 by shRNA significantly hindered cell viability, invasion, and migration in androgen receptor (AR)-positive bladder cancer cells [27]. In intrahepatic cholangiocarcinoma cells (ICC), the autocrine parathyroid hormone-like hormone (PTHLH) activated the ERK and JNK signaling pathway, which then upregulated ATF2 and cyclin D1 expression [26]. Recent researches discovered the critical functions of ATF2 in inflammation. For example, it was explored that ATF2 promoted mucosal damage and intestinal inflammation of the inflamed small intestine by targeting *Reg4* gene and enhancing its transcriptional expression [28]. Our previous study detected a high expression and phosphorylation of ATF2 in a neuroinflammatory model and proved the existence of TRAF6-JNK/p38-ATF2 axis in microglial inflammatory activation [18].

Implied by latest studies, ATF2 might be involved in RA circadian imbalance and hyperinflammation. CirRNA Hsa_circ_0001859 acted as a miRNA sponge to compete with ATF2 for miR-204/211 and thus elevated ATF2 expression and promoted inflammatory activity in SW982 cells [19]. Transcriptome and proteome analyses revealed a time-of-day variation in gene expression of PBML in RA patients, and *ex vivo* stimulation identified a time-of-day alteration of ATF2 phosphorylation level in RA [20]. However, the expression of ATF2 protein in synovium tissues of RA and its potential regulatory function in RA-FLSs activation remained unclear. In the present experiment, we first investigated an increased expression and phosphorylation of ATF2 in both synovial tissues of RA patients and TNF-α-induced SW982 cells, which was used as an activated FLSs cell model. ATF2 knockdown not only led to a decrease of IL-6, IL-1β, and MMP-13 expression but also inhibited the cell migration and invasion in SW982 cells after TNF-α induction. These results indicated a critical contribution of ATF2 to RA-FLSs activation and synovial inflammation.

To further understand the upstream signaling pathway of ATF2 during RA-FLSs activation, we paid attention to Spry2-ERK. ERK MAPK is one of the well identified kinases which phosphorylate and activate ATF2 upon multiple extracellular stress stimulation. ERK pathway has been proved to be activated in RA-FLSs and thus play crucial activities in RA pathogenesis. Here, we indeed observed an elevated phosphorylation of ERK in the synovium tissues of RA patients and TNF-α treated SW982 cells.

SPRY2 belongs to the sprouty protein family (SPRY1-4) and negatively regulates receptor tyrosine kinase (RTK) and ERK MAPK signaling [29]. The down-regulation of SPRY2 expression was observed in a series

of tumors including coloanal, hepatocellular, lung, prostate, and breast cancers [30–32]. As a tumor suppressor, SPRY2 overexpression inhibits proliferation, migration, and invasion of several tumor cells. SPRY2 attenuates the ERK MAPK signaling by binding to and antagonizing the activities of RAF1, BRAF, and SYK in chronic lymphocytic leukemia (CLL) cells [33]. In gastric cancer, mir-592 promotes proliferation, migration, and invasion through the PI3K/AKT and MAPK/ERK signaling pathways by targeting SPRY2 [34]. Moreover, miR-27a promoted ERK phosphorylation by down-regulating SPRY2 in monocytes in liver inflammation [35]. These results confirmed the negative regulation of SPRY2 on ERK MAPK signaling pathway no matter in cancer or inflammation.

SPRY2-ERK MAPK axis also participates in RA inflammation. In 2015, SPRY2 was found to effectively reduce rat adjuvant-induced arthritis (AIA) inflammation by blocking AKT and ERK pathways, which was further confirmed by *in vitro* cell experiments [36]. Our team further revealed that Dyrk1A promoted the proliferation, migration, and invasion of FLSs by down-regulating SPRY2 expression [9]. In accordance with previous reports, we found a decreased SPRY2 expression in the synovium tissues of RA patients in this study. SPRY2 overexpression inhibited pro-inflammatory factors production, migration, and invasion of FLSs. More importantly, SPRY2 overexpression reduced phosphorylation of both ERK and ATF2 in TNF-α treated SW982 cells.

Taken together, our findings demonstrated that overexpression and activation of ATF2 greatly contributed to migration and invasion of RA-FLSs. SPRY2 might inhibit the inflammatory response of FLSs to extracellular stimuli by suppressing ERK MAPK-ATF2 signaling pathway. Either overexpressing SPRY2 or knocking down ATF2 may become hopeful novel therapeutic targets for manipulating RA-FLS activation. Further studies are required to extensively clarify the precise regulation of SPRY2-ERK-ATF2 cascade in FLSs and explore its potential value for RA treatments.

FUNDING INFORMATION

This work was supported by the National Natural Science Foundation of China (81702216), Scientific Research Project of “333 Project” in Jiangsu Province (BRA2018224), Nantong Science and Technology Project (JC2019031), Scientific Research Project of Health Commission of Jiangsu Province (H2018035).

COMPLIANCE WITH ETHICAL STANDARDS

Conflict of Interest. The authors declare that they have no conflict of interest.

REFERENCES

1. Okada, Y., D. Wu, G. Trynka, T. Raj, C. Terao, K. Ikari, Y. Kochi, K. Ohmura, A. Suzuki, S. Yoshida, R.R. Graham, and A. Manoharan. 2014. Genetics of rheumatoid arthritis contributes to biology and drug discovery[J]. *Nature* 506 (7488): 376–381.
2. Källberg, H., B. Ding, L. Padyukov, C. Bengtsson, J. Rönnelid, L. Klareskog, and L. Alfredsson. 2011. Null null. Smoking is a major preventable risk factor for rheumatoid arthritis: estimations of risks after various exposures to cigarette smoke[J]. *Annals of the Rheumatic Diseases* 70 (3): 508–511.
3. Konig, M.F., L. Abusleme, J. Reinholdt, R.J. Palmer, R.P. Teles, K. Sampson, A. Rosen, P.A. Nigrovic, J. Sokolove, and J.T. Giles. 2016. Aggregatibacter actinomycetemcomitans-induced hypercitrullination links periodontal infection to autoimmunity in rheumatoid arthritis[J]. *Science Translational Medicine* 8: 369ra176.
4. McInnes, I.B., and G. Schett. 2017. Pathogenetic insights from the treatment of rheumatoid arthritis[J]. *Lancet* 389: 2328–2337.
5. Ganesan, R., and M. Rasool. 2017. Fibroblast-like synoviocytes-dependent effector molecules as a critical mediator for rheumatoid arthritis: Current status and future directions[J]. *International Reviews of Immunology* 36 (1): 20–30.
6. Agere, S.A., N. Akhtar, J.M. Watson, and S. Ahmed. 2017. RANTES/CCL5 induces collagen degradation by activating MMP-1 and MMP-13 expression in human rheumatoid arthritis synovial fibroblasts [J]. *Frontiers in Immunology* 8: 1341.
7. Zou, Y., S. Zeng, M. Huang, Q. Qiu, Y. Xiao, M. Shi, Z. Zhan, L. Liang, X. Yang, and H. Xu. 2017. Inhibition of 6-phosphofructo-2-kinase suppresses fibroblast-like synoviocytes-mediated synovial inflammation and joint destruction in rheumatoid arthritis[J]. *British Journal of Pharmacology* 174 (9): 893–908.
8. Wang, H., S. Tu, S. Yang, P. Shen, Y. Huang, X. Ba, W. Lin, Y. Huang, Y. Wang, K. Qin, Chen Z. Berberine, and L.P.A. Modulates. 2019. Function to inhibit the proliferation and inflammation of FLS-RA via p38/ERK MAPK Pathway Mediated by LPA[J]. *Evidence-based Complementary and Alternative Medicine: Ecam* 2019: 2580207.
9. Guo, X., D. Zhang, X. Zhang, J. Jiang, P. Xue, C. Wu, J. Zhang, G. Jin, Z. Huang, J. Yang, X. Zhu, W. Liu, G. Xu, Z. Cui, and G. Bao. 2018. Dyrk1 A promotes the proliferation, migration and invasion of fibroblast-like synoviocytes in rheumatoid arthritis via down-regulating Spry2 and activating the ERK MAPK pathway[J]. *Tissue & Cell* 54: 63–70.
10. Shuang, F., Y. Zhou, S.X. Hou, J.L. Zhu, Y. Liu, C.L. Zhang, and J.G. Tang. 2015. Indian hedgehog signaling pathway members are associated with magnetic resonance imaging manifestations and pathological scores in lumbar facet joint osteoarthritis[J]. *Scientific Reports* 5: 10290.
11. Zhao, Q., S. Chen, Z. Zhu, L. Yu, Y. Ren, M. Jiang, J. Weng, and B. Li. 2018. miR-21 promotes EGF-induced pancreatic cancer cell

proliferation by targeting Spry2[J]. *Cell Death & Disease* 9 (12): 1157.
12. Xu, Y.F., H.D. Liu, Z.L. Liu, C. Pan, X.Q. Yang, S.L. Ning, Z.L. Zhang, S. Guo, and J.M. Yu. 2018. Sprouty2 suppresses progression and correlates to favourable prognosis of intrahepatic cholangiocarcinoma via antagonizing FGFR2 signalling[J]. *Journal of Cellular and Molecular Medicine* 22 (11): 5596–5606.
13. Zhang, W., Z. Du, J. Zhu, J. Yu, and Y. Xu. 2015. Sprouty2 suppresses the inflammatory responses in rheumatoid arthritis fibroblast-like synoviocytes through regulating the Raf/ERK and PTEN/AKT signals[J]. *Molecular Immunology* 67 (2 Pt B): 532–539.
14. Watson, G., Z.A. Ronai, and E. Lau. 2017. ATF2, a paradigm of the multifaceted regulation of transcription factors in biology and disease[J]. *Pharmacological Research* 119: 347–357.
15. Li, X.Y., and M.R. Green. 1996. Intramolecular inhibition of activating transcription factor-2 function by its DNA-binding domain[J]. *Genes & Development* 10 (5): 517–527.
16. Zhang, R., H. Luo, S. Wang, Z. Chen, L. Hua, H.W. Wang, W. Chen, Y. Yuan, X. Zhou, D. Li, S. Shen, T. Jiang, Y. You, N. Liu, and H. Wang. 2015. MiR-622 suppresses proliferation, invasion and migration by directly targeting activating transcription factor 2 in glioma cells[J]. *Journal of Neuro-Oncology* 121 (1): 63–72.
17. Wu, D.S., C. Chen, Z.J. Wu, B. Liu, L. Gao, Q. Yang, W. Chen, J.M. Chen, Y. Bao, L. Qu, and L.H. Wang. 2016. ATF2 predicts poor prognosis and promotes malignant phenotypes in renal cell carcinoma[J]. *Journal of Experimental & Clinical Cancer Research: CR* 35 (1): 108.
18. Li, M., D. Zhang, X. Ge, X. Zhu, Y. Zhou, Y. Zhang, X. Peng, and A. Shen. 2019. TRAF6-p38/JNK-ATF2 axis promotes microglial inflammatory activation[J]. *Experimental Cell Research* 376 (2): 133–148.
19. Li, B., N. Li, L. Zhang, K. Li, Y. Xie, M. Xue, and Z. Zheng. 2018. Hsa_circ_0001859 regulates ATF2 expression by functioning as an MiR-204/211 sponge in human rheumatoid arthritis[J]. *Journal of Immunology Research* 2018: 9412387.
20. Poolman, T.M., J. Gibbs, A.L. Walker, S. Dickson, L. Farrell, J. Hensman, A.C. Kendall, R. Maidstone, S. Warwood, and A. Loudon. 2019. Rheumatoid arthritis reprograms circadian output pathways[J]. *Arthritis Research & Therapy* 21 (1): 47.
21. Pfeifle, R., T. Rothe, N. Ipseiz, H.U. Scherer, S. Culemann, U. Harre, J.A. Ackermann, M. Seefried, A. Kleyer, and S. Uderhardt. 2017. Regulation of autoantibody activity by the IL-23-T17 axis determines the onset of autoimmune disease[J]. *Nature Immunology* 18 (1): 104–113.
22. Fessler, J., R. Husic, V. Schwetz, E. Lerchbaum, F. Aberer, P. Fasching, A. Ficjan, B. Obermayer-Pietsch, C. Duftner, and W. Graninger. 2018. Senescent T-cells promote bone loss in rheumatoid arthritis[J]. *Frontiers in Immunology* 9: 95.
23. Wu, S., Y. Li, L. Yao, Y. Li, S. Jiang, W. Gu, H. Shen, L. Xia, and J. Lu. 2018. Interleukin-35 inhibits angiogenesis through STAT1 signalling in rheumatoid synoviocytes[J]. *Clinical and Experimental Rheumatology* 36 (2): 223–227.
24. Zeke, A., M. Misheva, A. Reményi, and M.A. Bogoyevitch. 2016. JNK signaling: regulation and functions based on complex protein-protein partnerships[J]. *Microbiology and Molecular Biology Reviews* 80 (3): 793–835.
25. Colomb, F., M.A. Krzewinski-Recchi, A. Steenackers, A. Vincent, A. Harduin-Lepers, P. Delannoy, and S. Groux-Degroote. 2017. TNF up-regulates ST3GAL4 and sialyl-Lewisx expression in lung epithelial cells through an intronic ATF2-responsive element[J]. *The Biochemical Journal* 474 (1): 65–78.
26. Tang, J., Y. Liao, S. He, J. Shi, L. Peng, X. Xu, F. Xie, N. Diao, J. Huang, Q. Xie, C. Lin, X. Luo, K. Liao, J. Ma, J. Li, D. Zhou, and Z. Li. 2017. Autocrine parathyroid hormone-like hormone promotes intrahepatic cholangiocarcinoma cell proliferation via increased ERK/JNK-ATF2-cyclinD1 signaling[J]. *Journal of Translational Medicine* 15 (1): 238.
27. Inoue, S., T. Mizushima, H. Ide, G. Jiang, T. Goto, Y. Nagata, G.J. Netto, and H. Miyamoto. 2018. ATF2 promotes urothelial cancer outgrowth via cooperation with androgen receptor signaling[J]. *Endocrine Connections* 7 (12): 1397–1408.
28. Xiao, Y., Y. Lu, Y. Wang, W. Yan, and W. Cai. 2019. Deficiency in intestinal epithelial Reg4 ameliorates intestinal inflammation and alters the colonic bacterial composition[J]. *Mucosal Immunology* 12 (4): 919–929.
29. Yigzaw, Y., L. Cartin, S. Pierre, K. Scholich, and T.B. Patel. 2001. The C terminus of sprouty is important for modulation of cellular migration and proliferation[J]. *The Journal of Biological Chemistry* 276: 22742–22747.
30. Feng, Y.H., C.L. Wu, C.J. Tsao, J.G. Chang, P.J. Lu, K.T. Yeh, Y.H. Uen, J.C. Lee, and A.L. Shiau. 2011. Deregulated expression of sprouty2 and microRNA-21 in human colon cancer: Correlation with the clinical stage of the disease[J]. *Cancer Biology & Therapy* 11: 111–121.
31. Gao, M., R. Patel, I. Ahmad, J. Fleming, J. Edwards, S. McCracken, K. Sahadevan, M. Seywright, J. Norman, O. Sansom, and H.Y. Leung. 2012. SPRY2 loss enhances ErbB trafficking and PI3K/AKT signalling to drive human and mouse prostate carcinogenesis[J]. *EMBO Molecular Medicine* 4: 776–790.
32. Patel, R., M. Gao, I. Ahmad, J. Fleming, L.B. Singh, T.S. Rai, A.B. McKie, M. Seywright, R.J. Barnetson, J. Edwards, O.J. Sansom, and H.Y. Leung. 2013. Sprouty2, PTEN, and PP2A interact to regulate prostate cancer progression[J]. *The Journal of Clinical Investigation* 123: 1157–1175.
33. Shukla, A., K. Rai, V. Shukla, N.K. Chaturvedi, R.G. Bociek, S.J. Pirruccello, H. Band, R. Lu, and S.S. Joshi. 2016. Sprouty2: A novel attenuator of B-cell receptor and MAPK-Erk signaling in CLL[J]. *Blood* 127 (19): 2310–2321.
34. He, Y., Y. Ge, M. Jiang, J. Zhou, D. Luo, H. Fan, L. Shi, L. Lin, and L. Yang. 2018. MiR-592 promotes gastric cancer proliferation, migration, and invasion through the PI3K/AKT and MAPK/ERK signaling pathways by targeting Spry2[J]. *Cellular Physiology and Biochemistry: International Journal of Experimental Cellular Physiology, Biochemistry, and Pharmacology* 47 (4): 1465–1481.
35. Saha, B., J.C. Bruneau, K. Kodys, and G. Szabo. 2015. Alcohol-induced miR-27a regulates differentiation and M2 macrophage polarization of normal human monocytes[J]. *Journal of Immunology (Baltimore, Md. : 1950)* 194 (7): 3079–3087.
36. Zhang, W., J. Zhu, Z. Du, J. Yu, Y. Xu, and F. Wang. 2015. Intraarticular gene transfer of SPRY2 suppresses adjuvant-induced arthritis in rats[J]. *Applied Microbiology and Biotechnology* 99 (16): 6727–6735.